Immunity, Vol. 4, 421–430, May, 1996, Copyright ©1996 by Cell Press

Polarity of T Cell Shape, Motility, and Sensitivity to Antigen

Paul A. Negulescu,* Tatiana B. Krasieva,† Abrar Khan,*§ Hubert H. Kerschbaum,*‡ and Michael D. Cahalan*
*Department of Physiology and Biophysics
†Beckman Laser Institute
University of California, Irvine
Irvine, California 92717

Summary

T cell activation requires contact with APCs. We used optical techniques to demonstrate T cell polarity on the basis of shape, motility, and localized sensitivity to antigen. An intracellular Ca^{2+} clamp showed that T cell shape and motility are extremely sensitive to changes in $[Ca^{2+}]_i$ (K_d = 200 nM), with immobilization and rounding occurring via a calcineurin-independent pathway. Ca^{2+}-dependent immobilization prolonged T cell contact with the antigen-presenting B cell; buffering the $[Ca^{2+}]_i$ signal prevented the formation of stable cell pairs. Optical tweezers revealed spatial T cell sensitivity to antigen by controlling placement on the T cell surface of either B cells or α-CD3 MAb-coated beads. T cells were 4-fold more sensitive to contact made at the leading edge of the T cell compared with the tail. We conclude that motile T cells are polarized antigen sensors that respond physically to $[Ca^{2+}]_i$ signals to stabilize their interaction with APCs.

Introduction

T cells carry out immune surveillance in vivo by periodically exiting the bloodstream and circulating through tissues. Contact of a single T cell with an appropriate antigen-presenting cell (APC) initiates a biochemical cascade through the T cell antigen receptor (TCR), which leads to clonal expansion and, ultimately, an immune response. The physical nature of T cell activation by APCs differs from cell activation by soluble factors in that both T cell shape and the orientation of the T cell–B cell pair may affect the cellular response. Furthermore, feedback between shape and receptor-mediated signals could influence the cellular response by modulating both immune surveillance and cell–cell interactions. These considerations raise two questions about the genesis of the immune response: do second messengers generated by T cell activation influence the behavior of T cells in either the absence or presence of B cells; and, what are the contact requirements for T cell activation by B cells?

T cell polarity following contact with an APC has been well characterized on the basis on plasma membrane protein clustering (Kupfer and Singer, 1989), cytoskeletal and organellar reorganization (Kupfer et al., 1986; Lee et al., 1988), and cytokine secretion. These changes occur over hours and promote the activation of specific cells in crowded environments such as lymph nodes, where most antigen is detected (Poo et al., 1988; Kupfer et al., 1994). In addition to reorganization triggered by cell–cell contact, T cells are motile and therefore possess some inherent polarity even before they engage the APC (Stossel, 1993; Agarwal and Linderman, 1995). The role of inherent polarity in T cell activation has not been determined.

$[Ca^{2+}]_i$ is an important second messenger leading to T cell activation (Crabtree and Clipstone, 1994). A rise in $[Ca^{2+}]_i$ can initiate several intracellular pathways, including the activation of interleukin-2 (IL-2) gene transcription via calcineurin, a Ca^{2+}-dependent phosphatase. Calcineurin activity dephosphorylates a cytoplasmic component of nuclear factor of activated T cells (NF-AT), allowing its transport to the nucleus where it promotes expression of the IL-2 gene. The link between Ca^{2+} and an NF-AT-driven IL-2 reporter gene has been quantified at the level of individual cells (Negulescu et al., 1994). In addition to regulating transcriptional events, $[Ca^{2+}]_i$ has effects on leukocyte behavior. For example, $[Ca^{2+}]_i$ elevation stimulates eosinophil and neutrophil chemotaxis (Brundage et al., 1991; Maxfield, 1993; Mandeville et al., 1995) and causes rounding in T cells (Donnadieu et al., 1994). However, little is known about the dynamic control of T cell morphology by $[Ca^{2+}]_i$ or its role in coordinating cell–cell contact.

We resolved the relationships among T cell behavior, $[Ca^{2+}]_i$, and antigen presentation using optical techniques to measure and manipulate activation of highly responsive antigen-specific murine T cells. A two-camera video-imaging system simultaneously recorded both cell morphology and $[Ca^{2+}]_i$, while optical tweezers permitted localized mapping of T cell responsiveness to a complementary antigen-presenting B cell line or to antibody-coated beads. By combining functional assays of cell shape and $[Ca^{2+}]_i$, we show how the physical aspects of T cell activation and $[Ca^{2+}]_i$ signaling patterns are linked during the first moments of an immune response.

Results

This paper relates intracellular signaling patterns to T cell behavior. To help convey the dynamic nature of these data, we have made digital videos from several experiments available on the internet. By accessing our server at http://www.cell.com/Immunity (see Experimental Procedures), the reader can compare data shown in a given figure with a time-lapse version of the original experiment.

$[Ca^{2+}]_i$ Controls the Motility and Shape of T Cells

Temperature Dependence of T Cell Behavior on Glass

When settled onto coverglass at room temperature, 1E5 cells adhered poorly, appeared round, and displayed

‡Current address: Department of Physiology, Institute for Zoology, University of Salzburg, 5020 Salzburg, Austria.
§Current address: Department of Surgery, Henry Ford Hospital, Detroit, Michigan, 48202.

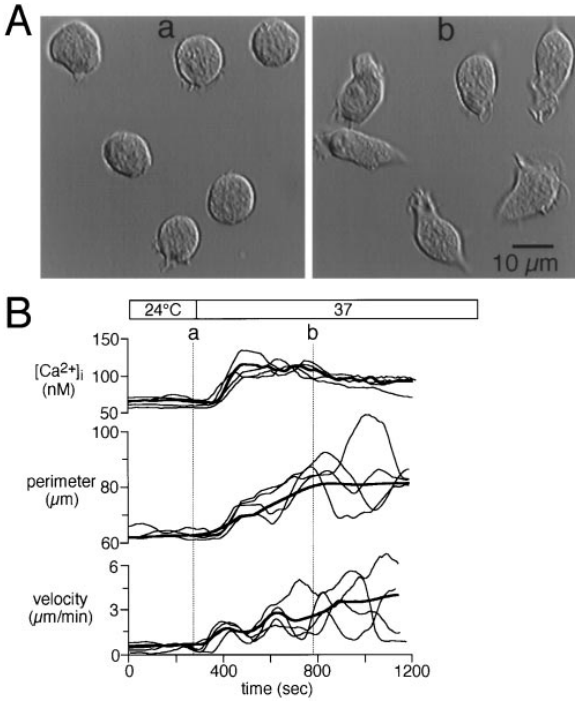

Figure 1. Temperature Dependence of Shape and Motility in 1E5 T Cells

(A) DIC images of cells at 24°C (a) and after 8 min at 37°C (b).
(B) Parallel measurements of $[Ca^{2+}]_i$, perimeter, and velocity during the temperature shift. The stage was heated at the time indicated. Note the incease in both cell perimeter and crawling velocity at 37°C. Thin lines, four individual cells from (A). Thick lines, average from all cells in (A). Time markers (a–b) correspond to images in (A). Experiment is typical of five similar experiments.

few processes. However, when warmed to 37°C, these cells adhered to the glass, extended a fan-shaped flattened leading edge in the direction of travel, and began to crawl. Figure 1 shows that this transition occurred within 1 min of warming and was complete in 5–10 min. Polarized cell shapes and crawling were observed in ~90% of the cells at 37°C. Shape changing comprised a repetitive cycle of rounding and elongating with a period of 1–5 min. The shape cycle, consisting of the extension of a thin organelle-free leading edge followed by the retraction of the thicker tail (uropod), was tracked by measuring either cell perimeter (Figure 1B) or an index of shape (see Figure 2). Cells crawled at varying rates but averaged 4.5 μm/min (Figure 1B) and, unless perturbed, generally moved in either straight or gently curving paths (see Figure 3). Although warming the cells caused a small increase in basal $[Ca^{2+}]_i$ (from 60 nM to 90 nM), shape changes associated with crawling occurred without detectable $[Ca^{2+}]_i$ fluctuations under control conditions.

$[Ca^{2+}]_i$ Dependence of T Cell Shape, Motility, and Immobilization

The microsomal Ca^{2+} pump inhibitor thapsigargin (TG) depletes intracellular Ca^{2+} stores (Thastrup et al., 1989) and subsequently induces Ca^{2+} influx into lymphocytes (Gouy et al., 1991) through Ca^{2+}-selective channels (Zweifach and Lewis, 1993). TG addition to 1E5 cells caused a $[Ca^{2+}]_i$ rise followed by rounding and immobilization (Figure 2). Figure 2 shows the effect of raising $[Ca^{2+}]_i$ on shape at various times during the experiment. TG increased $[Ca^{2+}]_i$ to a stable plateau of 600 nM within 60 s. Within 10 s of the $[Ca^{2+}]_i$ rise, motility decreased, and the cell was completely immobile within 30 s. Elevation of $[Ca^{2+}]_i$ also preceded cell rounding (Figures 2A and 2B) as reflected by a decrease in shape index (from ~2.5–1; see Experimental Procedures). Rounding began within 15 s and was complete within 150 s of the sustained $[Ca^{2+}]_i$ rise. Once cell shape stabilized, the cell surface was smooth, and showed little detectable motion. The original elongated shape was restored by lowering $[Ca^{2+}]_i$ using high extracellular $[K^+]$ solution to depolarize the membrane potential and thereby reduce Ca^{2+} influx. A second shape cycle was triggered in the same cell by a second $[Ca^{2+}]_i$ increase in low $[K^+]$ (Figures 2Af and 2B). The kinetics of Ca^{2+}-driven shape changes indicate that the fastest possible cycle from a fully elongated crawling cell to a completely round immobilized cell and back is ~5 min. However, Figure 2 shows that partial shape transitions are detectable within seconds of changes in $[Ca^{2+}]_i$. The time course of shape recovery was independent of either the magnitude or duration of the $[Ca^{2+}]_i$ rise; cells always began elongating within ~1 min of lowering $[Ca^{2+}]_i$. In contrast, the recovery of crawling was dependent on both the duration and magnitude of the $[Ca^{2+}]_i$ pulse. In control experiments, high $[K^+]$ solutions of up to 45 mM had no effect on shape or motility before TG addition, indicating that crawling and shape are independent of membrane potential. Conversely, TG did not induce shape changes in Ca^{2+}-free solutions. These results indicate that $[Ca^{2+}]_i$ elevation rapidly causes rounding and immobilization in T cells. $[Ca^{2+}]_i$ regulation of T cell shape and motility was unaffected by inhibition of the Ca^{2+}-dependent phosphatase calcineurin, since addition of 200 nM cyclosporin A did not inhibit the effects of TG (Table 1).

We determined the $[Ca^{2+}]_i$ dependence of both T cell shape and motility with a $[Ca^{2+}]_i$ clamp method in which TG-treated 1E5 cells are maintained at various $[Ca^{2+}]_i$ with extracellular solutions containing different $[K^+]$ (Negulescu et al., 1994). Figure 2C shows how 43 cells responded to $[Ca^{2+}]_i$ in eight experiments. At resting $[Ca^{2+}]_i$ (~80 nM) the shape index was randomly distributed between 1.3–2.6, reflecting the variety of shapes associated with crawling. The variation in shape decreased steeply between 150–500 nM $[Ca^{2+}]_i$ as the average cell became round. Blebbing occurred above 700 nM $[Ca^{2+}]_i$. The dependence of cell crawling on $[Ca^{2+}]_i$ was fitted to a Hill equation with coefficient of 3.5 and a K_d of 200 nM $[Ca^{2+}]_i$. These results indicate a highly sensitive, rapidly responsive, reversible mechanism coupling T cell behavior to $[Ca^{2+}]_i$ changes in the 150–300 nM range.

Directional Control by $[Ca^{2+}]_i$

Since the leading edge determined the direction of T cell motility and a $[Ca^{2+}]_i$ rise caused a reversible loss of polarized appearance, we evaluated the consequences of varying $[Ca^{2+}]_i$ on the direction of travel. Trails from 36 individual cells treated with TG in several different $[K^+]$ solutions were analyzed and grouped into one of three categories based on whether they continued in their original direction (<30 degree change),

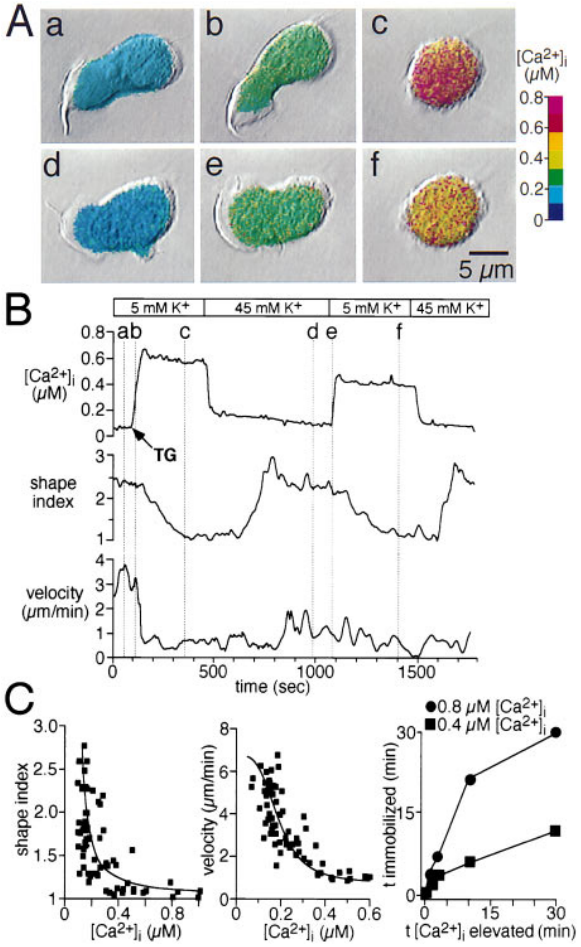

Figure 2. Elevated $[Ca^{2+}]_i$ Alters Cell Morphology and Inhibits Motility in 1E5 T Cells

(A) Overlay of TG (0.5 μM)-induced morphology and $[Ca^{2+}]_i$ change. Video available.

(B) Correlation of $[Ca^{2+}]_i$ with morphology and motility in same cell as part (A). Note rounding (shape index of circle is 1) and retraction of leading edge in high $[Ca^{2+}]_i$ and the reversibility of cell rounding in 45 mM extracellular $[K^+]$. The velocity change was not fully reversible due to the magnitude of the $[Ca^{2+}]_i$ signal. Time markers (a–f) correspond to images (a–f) in (A).

(C) Summary of $[Ca^{2+}]_i$ dependences for shape (left), motility (center), and immobilization (right). For shape (n = 67 cells, eight experiments) and motility (n = 58 cells, five experiments), each point represents a single cell clamped for 6 min at the indicated $[Ca^{2+}]_i$. Some cells were clamped at multiple $[Ca^{2+}]_i$. Shape index curve was drawn by hand. Velocity (v) versus $[Ca^{2+}]_i$ data were fitted a Hill equation $v = v_{min} + v_{max} / [1 + ([Ca^{2+}]_i/K_d)^n]$, where v_{max} is the maximum velocity (6.5 μm/min), K_d (200 nM) is the half-maximal $[Ca^{2+}]_i$ concentration required to immobilize cells, and n is the Hill coefficient (3.5). v_{min} of 0.75 μm/min represents a minimum velocity due to mechanical drift or small changes in shape. To determine the time of immobilization, cells were treated with TG in either 22 mM or 5 mM $[K^+]$ to produce $[Ca^{2+}]_i$ of either 0.4 μM (squares) or 0.8 μM (circles), respectively. The duration of elevated $[Ca^{2+}]_i$ was varied by changing the interval between TG addition in low $[K^+]$ and high $[K^+]$ addition. Time immobilized was measured from the time $[Ca^{2+}]_i$ was lowered (in 45 mM $[K^+]$) to the time cells moved one cell diameter (~12 μm) from their immobilized position. These results contrast with the $[Ca^{2+}]_i$ dependence of shape and suggest that 1E5 cells begin adhering to glass above 0.4 μM $[Ca^{2+}]_i$.

turned (>30 degree change), or stopped crawling. Four examples of each type of response are shown in Figure 3A. Cell trails have been rotated and aligned to cross the horizontal axis at the moment of TG addition. The averaged $[Ca^{2+}]_i$ signals from all cells associated with each type of response are plotted in Figure 3B. T cell motility responded in distinct ways to $[Ca^{2+}]_i$ signals of increasing magnitude. Small brief $[Ca^{2+}]_i$ transients peaking around 400 nM and lasting ~1 min caused only a pause in motility, as seen by the clustering of points in the "no turn" group shortly after TG addition. A medium-sized $[Ca^{2+}]_i$ pulse to ~600 nM lasting ~2–3 min caused ~70% of the cells to change direction. The initial peak of this $[Ca^{2+}]_i$ pulse was of sufficient magnitude and duration to cause a transient retraction of the leading edge (see also Figure 2), but the sustained level of about 300 nM permitted the formation of a new leading edge corresponding to a new direction of travel. A larger $[Ca^{2+}]_i$ increase to 800 nM, which relaxed to a plateau at about 500 nM, immobilized the cells.

Shape and Motility of Human T Cells

Resting human T cells were generally round and immobile at 37°C (data not shown). However, phytohemagglutinin-stimulated human T cells (lymphoblasts) showed dynamic shape patterns that were identical to 1E5 cells. On average, TG-stimulated $[Ca^{2+}]_i$ elevation decreased the average shape index of activated human T cells from 2.1 to 1.1 (n = 16 cells; Table 1), and this decrease was reversed in 45 mM $[K^+]$.

$[Ca^{2+}]_i$ Signals and T Cell–B Cell Contact during Antigen Presentation

Three Stages of T–B Contact

We examined the role of $[Ca^{2+}]_i$ in T cell–B cell contact by tracking the interaction of hen egg lysosome (HEL)-specific 1E5 cells and a conjugate B cell line (2PK3). Although B cells were able to extend and retract processes, they were generally round, immobile, showed no $[Ca^{2+}]_i$ rise, and exhibited relatively subtle shape changes when presenting antigen to T cells. We therefore describe the contact pattern with reference to T cell behavior. Typically, the crawling T cell made brief (20–60 s) probing contact via a thin organelle-free leading edge with the B cell (Figure 4Aa). In the case of contact with either another T cell or a naive (i.e., nonantigen pulsed) B cell (Figure 4Aa–d), the T cell continued crawling (Figure 4Ab), ending contact within 2–10 min (Figures 4Ad and 4B). In contrast, T cells that encountered antigen-presenting B cells began a program lasting >20 min and consisting of three distinct stages, which we termed contact, recognition, and stabilization (Figures 4Ae–h and 4C).

The contact phase lasted from 20 s to several minutes and consisted of T cell probing and contact with the B cell prior to any change in $[Ca^{2+}]_i$. This phase is similar to contact with naive B cells in that the thin-leading edge of the T cell probes the B cell (Figures 4Aa and 4Ae). We noticed that T cells on glass preferentially engaged B cells with this leading edge, rather than the thicker trailing edge (see below). When T cells contacted antigen-presenting B cells with the leading edge, progression through the next phases (determined in part

Table 1. Effects of TG and Cyclosporin A on T Cell $[Ca^{2+}]_i$, Shape, and Motility

Condition	Morphology		
	Shape index	Motility (μm/min)	$[Ca^{2+}]_i$ (μM)
1E5 cells			
Control	2.0 ± 0.5	4.3 ± 0.9	0.08 ± 0.03
45mM K^+	1.9 ± 0.3	4.8 ± 0.7	0.06 ± 0.02
TG (500 nM)	1.1 ± 0.1*	0.7 ± 0.4*	0.73 ± 0.18*
TG/45mM K^+	1.8 ± 0.6	3.9 ± 0.6	0.10 ± 0.05
TG + CsA	1.1 ± 0.2*	0.8 ± 0.2*	0.78 ± 0.13*
CsA (200 nM/30 min)	1.9 ± 0.5	4.0 ± 0.5	0.09 ± 0.02
Human T lymphoblasts			
Control	2.1 ± 0.6	ND	0.07 ± 0.02
TG (500 nM)	1.1 ± 0.1*	ND	0.64 ± 0.18*

Values represent mean ± SD of at least 20 cells on untreated glass in three experiments. Unless otherwise indicated, all values were obtained 15 min after drug addition. Cyclosporin A (200 nM) was added 30 min before TG addition. Asterisk indicates a value significantly different ($p < 0.005$) than control. Velocity measurements were not made on human T lymphoblasts (ND).

by increased $[Ca^{2+}]_i$; see below) occurred about 90% of the time (46 of 51 experiments).

Recognition lasted from 1–3 min and was the most dynamic stage of the interaction. This phase consisted of two nearly simultaneous events that indicate specific T cell recognition of the B cell. First, the T cell accelerated toward, increased contact with, and engulfed a portion of the B cell. Engulfing often involved about half of the surface of a B cell (Figure 4Af) and generated enough force to move the B cell. The second event was a T cell $[Ca^{2+}]_i$ transient, which usually began 7–15 s after the T cell began expanding its contact with the B cell, and peaked at ~1 μM around the time of maximum engulfing. Neither $[Ca^{2+}]_i$ increases nor engulfing were ever observed when T cells contacted naive B cells.

The third phase (stabilization) occurred after $[Ca^{2+}]_i$ had relaxed from peak levels and was characterized morphologically by a partial retraction of the engulfing

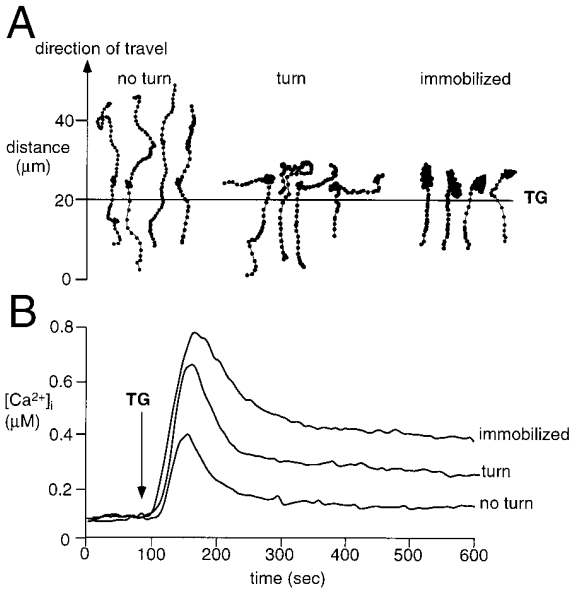

Figure 3. Directional Control of T Cell Motility by $[Ca^{2+}]_i$ Elevation

(A) Cell trails from 12 single cells grouped according to their directional response following a TG-induced $[Ca^{2+}]_i$ increase. Trails have been rotated so that all cells appear to move in the same direction before TG addition (indicated by the horizontal line). Examples in turn group chosen for clarity.

(B) Average $[Ca^{2+}]_i$ responses from all cells within each category (37 cells from six experiments).

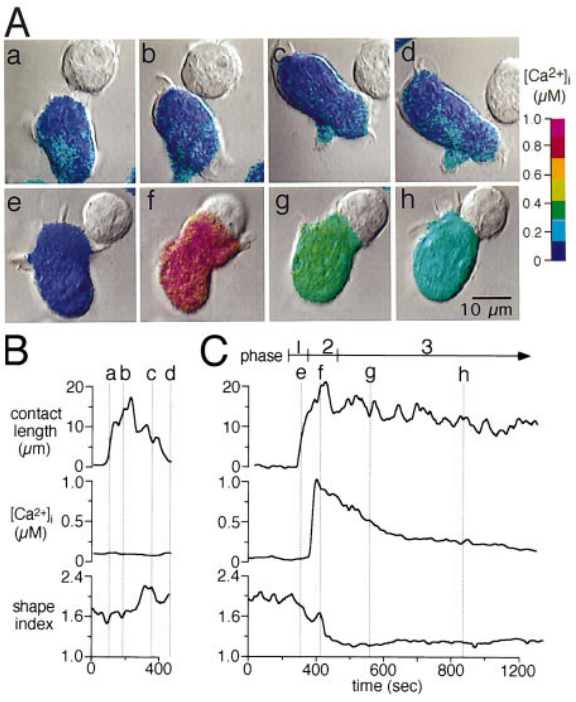

Figure 4. Correlation of $[Ca^{2+}]_i$ and T Cell Shape during Antigen Presentation

(A) Images of T–B cell contact and T cell $[Ca^{2+}]_i$ at various times following contact with B cells. Either naive (Aa–d) or B cells presenting HEL peptide (Ae–h, video available) were settled onto a coverglass with adherent fura-2-loaded T cells.

(B, C) Time course of $[Ca^{2+}]_i$ and cell–cell contact length from the same experiments as in (A). Note the engulfing, cell rounding, and prolonged contact when T cell contacts APC (C). Phases 1, 2, and 3 in (C) refer to contact, recognition, and stabilization phases of the interaction, respectively. Phase 1 is shown in Ae, phase 2 is shown in Af, and phase 3 progression is shown in Ag–h.

T cell from the B cell and subsequent rounding of the T cell (Figure 4Ag). This phase lasted about 5–10 min. Although the T cell decreased its contact surface with the B cell during the retraction, the pair was stable as long as $[Ca^{2+}]_i$ remained above baseline. In addition, T cells remained monogamous and did not seek to engage late-arriving B cells while $[Ca^{2+}]_i$ was elevated. B cells, in contrast, were promiscuous, often becoming simultaneously or sequentially engaged by several T cells.

The first three phases occurred regularly and represent a uniform pattern during the first 10–15 min of T cell contact with the APC. Following this rigid program, T cell behavior became heterogeneous as the waning $[Ca^{2+}]$ signals corresponded to new probing by the T cell and weaker cell–cell associations. During the variable phase, cells either maintained a relatively stable rounded shape, with moderately high $[Ca^{2+}]_i$ (about 30% of cells; see Figure 4A), or showed a more dynamic contact corresponding with erratic $[Ca^{2+}]_i$ spikes (55%; see Figure 5), or demonstrated no prolonged $[Ca^{2+}]_i$ signal and disengaged from the B cell (15%; data not shown).

$[Ca^{2+}]_i$ Influences T–B Contact Pattern during Antigen Presentation

$[Ca^{2+}]_i$ Oscillations Correlate with Shape Changes during Antigen Presentation

The unstable contact pattern observed during weak $[Ca^{2+}]_i$ signals (Figure 5) contrasts with the stable interaction that accompanied a prolonged $[Ca^{2+}]_i$ rise (see Figure 4). At first, the T cell in Figure 5 follows the typical pattern of contact, recognition, initial $[Ca^{2+}]_i$ rise, and rounding. However, as $[Ca^{2+}]_i$ rapidly decreases from peak toward resting levels, the contact patch destabilizes and the T cell moves around the B cell. More robust periods of $[Ca^{2+}]_i$ spike activity preceded a transient rounding and reorientation of the T cell toward the B cell (Figure 5Ab–c). In contrast, the brief period of small oscillations (Figure 5Ad–f) did not cause significant shape change. Ultimately, this pair was separated by a second T cell (data not shown). We noted that unstable pairs tended to have smaller and less persistent $[Ca^{2+}]_i$ signals. On average, there was a positive correlation between shape and $[Ca^{2+}]_i$ during the first 20 min of antigen presentation, such that cells with higher $[Ca^{2+}]_i$ signals were rounder (Figure 5C) and therefore formed more stable pairs. Figure 5C includes data from experiments in which $[Ca^{2+}]_i$ signals were blocked by cytoplasmic buffering (see below).

Intracellular $[Ca^{2+}]_i$ Bufferin

$[Ca^{2+}]_i$ signals during antigen presentation were blocked by exposure to high $[K^+]$ solutions and loading with the cytoplasmic Ca^{2+} buffer, BAPTA/AM (10 μM). This regime allowed cells to retain elongated shapes and crawl normally but greatly diminished the $[Ca^{2+}]_i$ response induced by antigen presentation (Figures 6A and 6B). These T cells made initial contact and engulfed antigen-presenting B cells but, in the absence of a $[Ca^{2+}]_i$ signal, did not round up or establish stable contact and often engaged a second B cell (Figure 6Ac). The Ca^{2+} requirement for stable contact with a single APC was demonstrated by repolarizing the membrane potential with normal low $[K^+]$ solution to raise $[Ca^{2+}]_i$. Figure 6B shows the

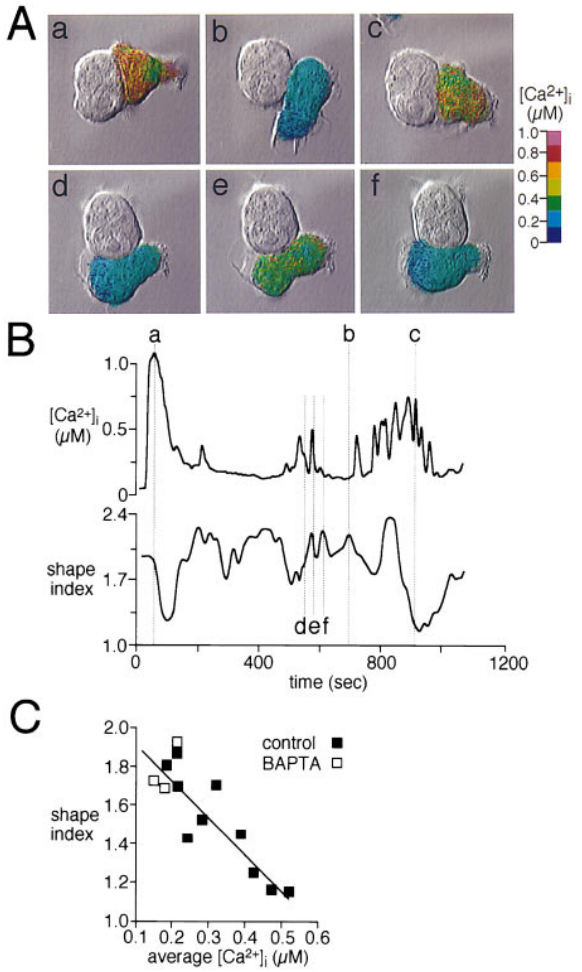

Figure 5. Unstable Contact Pattern in Cell with Oscillating $[Ca^{2+}]_i$ Signal

(A) Images of T–B cell contact and T cell $[Ca^{2+}]_i$ at various times following contact with a B cell. About 60% of T cells showed $[Ca^{2+}]_i$ oscillations after contact with antigen-presenting B cells.

(B) Correlation of cell shape and $[Ca^{2+}]_i$. If the oscillations are large or occur with high frequency (e.g., between b–c) the cell rounds and retracts processes. Small or infrequent oscillations (e.g., between e–g) do not influence shape. Video available.

(C) T cell shape correlates with intensity of $[Ca^{2+}]_i$ signal during antigen presentation. Shape and $[Ca^{2+}]_i$ signals from 13 experiments were averaged over 20 min following contact. Closed squares are control; open squares are from cells buffered with BAPTA and 45 mM external $[K^+]$.

transition from erratic shape changes in $[Ca^{2+}]_i$-buffered cells to stable shape induced by a $[Ca^{2+}]_i$ rise. Thus, the $[Ca^{2+}]_i$ signal appears necessary for progression from recognition to stabilization phases. Without it, the cell either loops through the engulfing/recognition program or abandons its target and attempts to engage another B cell.

T Cell Sensitivity to Antigen Localized by Optical Trapping

Observation of 68 random T–B interactions suggested that T cells that intitially contacted B cells with their leading edge usually (90%, see above) generated $[Ca^{2+}]_i$

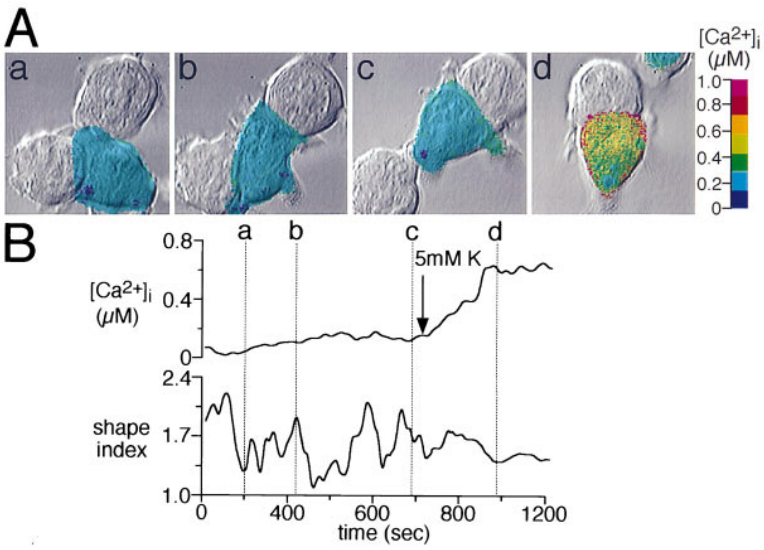

Figure 6. $[Ca^{2+}]_i$ Buffering Prevents Stable Cell–Cell Contact

(A, B) BAPTA-loaded T cell is an unstable partner until the $[Ca^{2+}]_i$ rise. T cells were loaded with both fura-2 and 10 μM BAPTA/AM and placed in solution containing 90 mM $[K^+]$, preventing most of the $[Ca^{2+}]_i$ increase triggered by contact with the B cell.

(A) Images of one T cell and two B cells.

(B) Analysis of shape and $[Ca^{2+}]_i$ from T cell in (A). The T cell engaged the first B cell (a), but with no $[Ca^{2+}]_i$ signal, contact was unstable and the T cell eventually moved to a second B cell (b–d). The $[Ca^{2+}]_i$ signal was initiated by returning cells to normal 5 mM $[K^+]$ solution. Note retraction of leading edge and more stable shape after $[Ca^{2+}]_i$ rise in (d). Video available.

responses, while T cells contacting B cells with their tails had only a 17% chance (3 of 17) of progressing past the contact phase. We tested the hypothesis that T cell responsiveness to B cells was polarized by using a laser-based optical trap to control the point of initial cell–cell contact while measuring T cell $[Ca^{2+}]_i$. As shown in Figure 7, when the B cell was placed at the T cell tail, no $[Ca^{2+}]_i$ response occurred (Figures 7Aa and 7B), and the B cell detached from the T cell within 2 min. However, trapping the loose B cell and placing it at the leading edge of the same T cell rapidly elicited a T cell $[Ca^{2+}]_i$ increase (Figures 7Ab and 7B). The $[Ca^{2+}]_i$ responses correlated with morphological changes in the T cell. For example, T cells would orient toward, increase contact with, and engulf B cells placed at the leading edge. In contrast, T cells making contact with B cells via the trailing edge showed little morphology change. T cell–B cell contact during antigen presentation involves intercellular interactions between a number of molecular pairs (Clark and Ledbetter, 1994), any of which could contribute to the observed polarity. To investigate whether polarity could be observed via TCR engagement alone, we used beads coated with antibodies to the CD3 subunit of the TCR complex to mimic TCR engagement in the absence of any coreceptors.

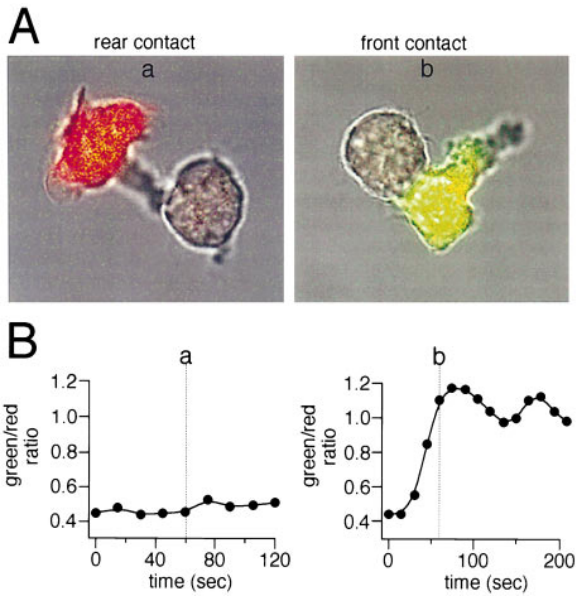

Figure 7. Optical Trapping of B Cell Reveals Functional T Cell Polarity

(A) Brightfield fluorescence overlays of T–B pairs with B cell trapped at either the tail (a) or leading edge (b) of the T cell. Colors are true-color emission shifts from fluo-3 and fura-red coloaded into 1E5 cells (red, low $[Ca^{2+}]_i$; yellow, high $[Ca^{2+}]_i$; see Experimental Procedures).

(B) Time course of fluo-3/fura-red intensity ratios for cells shown in (A). Experiment is representative of 15 runs). Ratio is directly proportional to $[Ca^{2+}]_i$.

The results from 29 T cell–B cell pairs and 32 bead–T cell pairs are summarized in Table 2, which shows similar functional polarity when using either B cells or α-CD3-coated beads to stimulate the T cell. T cells that were presented either antigen or beads at the leading edge (contact zone 1) had a higher probability of responding and a shorter latency of response than those contacting with their tail (contact zone 3). The longer latency seen in the tail responders could usually be attributed to the T cell reorienting its leading edge around to contact B cell or bead. Such gymnastics were not very effective, however, since about 50% of B cells or beads placed at the rear of the T cell eventually detached from the T cell. Based on the $[Ca^{2+}]_i$ signal as a funtional read-out, these data indicate that orientation of the leading edge of the T cell toward the APC is a critical element of successful antigen presentation. Our experiments with α-CD3-coated beads demonstrate that signaling initiated through the TCR alone exhibits the same polarity.

Discussion

Our results from video-imaging and cell-trapping experiments show that $[Ca^{2+}]_i$ signaling patterns regulate the shape and motility of single T cells. Furthermore, $[Ca^{2+}]_i$

Table 2. Polarized T Cell Response to TCR Stimulation

Contact zone (on T cell)	Cells responding (%)		Latency (sec)	
	B cell	α-CD3-bead	B cell	α-CD3-bead
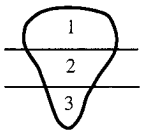				
1	82 (14/17)	90 (9/10)	42 ± 16	37 ± 15
2	80 (4/5)	67 (6/9)	63 ± 22	46 ± 26
3	31 (4/13)	22 (3/14)	146 ± 29	160 ± 32

T cells were stimulated by either antigen-presenting B cells or α-CD3ε-coated beads at the region indicated. Region 1 is defined as the leading edge. Latency indicates the delay between contact and a detectable Ca^{2+} increase in the responding population.

signals are necessary for normal T cell–B cell contact patterns during antigen presentation. Significantly, we use $[Ca^{2+}]_i$ signals to demonstrate a functional parallel between the morphological polarity of the T cell and its sensitivity to antigen. The importance of T cell shape is clear when one considers that lymphocytes adhere to cellular and extracellular matrices, squeeze through blood vessel fenestrations, and are usually activated in the packed cellular environment of lymph nodes (Springer, 1994). We propose that the T cell is a complex polarized sensor, spatially sensitive to external signals and able to alter its form in response to internal cues.

$[Ca^{2+}]_i$ Regulates T Cell Shape and Motility

Using a T cell line and a novel Ca^{2+} clamp technique, we determined that T cell shape and motility are steeply, rapidly, and reversibly sensitive to a rise in $[Ca^{2+}]_i$ with a K_d of ~200 nM (Figure 2C). Adhesion may involve a separate process because it required higher $[Ca^{2+}]_i$ and responded to longer signal durations. Our measurements of the kinetics and K_d of Ca^{2+}-triggered shape changes predict that physiological $[Ca^{2+}]_i$ oscillations that have a frequency between 0.1–1.5/min and reach levels ~1 μM (Donnadieu et al., 1992, Negulescu et al., 1994) would cause shape oscillations. This prediction is supported by our measurements of T cell shape and $[Ca^{2+}]_i$ during antigen presentation. Although freshly isolated human peripheral T cells are spherical and immobile, the transition to irregular changing shapes can be triggered by either adhesion to cellular monolayers (Arencibia et al., 1987), binding to extracellular matrix ligands (Shimizu and Shaw, 1991), and stimulation by chemokines (Tan et al., 1995, del Pozo et al., 1995) or mitogens (Thorpe et al., 1994, Donnadieu et al., 1994). The crawling polarized T cell hybridoma used here had properties similar to other T cell lines (data not shown) and phytohemagglutinin-activated human T cells (Table 1) and may be analogous to migrating or partially activated T cells in vivo. A relation between $[Ca^{2+}]_i$ and shape was shown by Donnadieu and coworkers (1992), who described first a permissive and later a causal (Donnadieu et al., 1994) role for elevated $[Ca^{2+}]_i$ in T cell rounding. Their work also established paradigms for relating shape, and $[Ca^{2+}]_i$ and cell activation.

With regard to the direction of crawling, our analysis suggests that T cells possess an integrating mechanism that translates control of cell shape into directional changes depending on the intensity of the $[Ca^{2+}]_i$ stimulus (Figure 3). For example, a cell exhibiting a small $[Ca^{2+}]_i$ signal pauses but, without full retraction of the leading edge, does not change its direction. A medium-sized $[Ca^{2+}]_i$ transient sufficient to retract the edge resets the direction of travel by permitting the formation of a new leading edge. Larger sustained $[Ca^{2+}]_i$ signals inhibit crawling by blocking shape changes and new edge formation. $[Ca^{2+}]_i$- and time-dependent adhesion, possibly mediated by integrins (Sjaastad et al., 1994), would also contribute to immobilization and allow the cell to "remember" the signal intensity. In a broad context, $[Ca^{2+}]_i$ control of shape and motility may serve an integrating function leading to excitation or inhibition depending on the site and origin of the signal. For example, near the site of antigen $[Ca^{2+}]_i$ signals could amplify an immune response. In contrast, immobilization elsewhere would suppress the immune response by limiting T cell surveillance.

Intracellular $[Ca^{2+}]_i$ gradients have been proposed to mediate directional control in eosinophils (Brundage et al., 1991). We did not detect $[Ca^{2+}]_i$ gradients underlying either polarity or motility in lymphocytes. The $[Ca^{2+}]_i$ dependence of lymphocyte motility is opposite to that described for other leukocytes where $[Ca^{2+}]_i$ increases are associated with increased motility. For example, $[Ca^{2+}]_i$ elevation speeds up neutrophil migration on various substrates (Mandeville et al., 1995) via a calcineurin-dependent mechanism (Hendey et al., 1992). The inhibition of T cell crawling by elevated $[Ca^{2+}]_i$ that occurred on glass did not require calcineurin and may indicate a substrate-independent mechanism. It will be important to see how T cell shape, motility, and adhesion patterns are affected by various extracellular matrices.

Second Messenger Control of T Cell Shape Is Distinct from Regulation of Gene Expression

Four findings indicate that the intracellular mechanisms controlling shape are distinct from those regulating gene expression (Negulescu et al., 1994). First, both shape and motility changes were unaffected by cyclosporin (Table 1), an inhibitor of the Ca^{2+}-dependent phosphatase, calcineurin, which is a key intermediate leading to IL-2 gene expression (Crabtree and Clipstone, 1994). Second, the $[Ca^{2+}]_i$ sensitivity of ~200 nM for shape changes is much less than the 1 μM required for NF-AT-driven gene expression. Third, small $[Ca^{2+}]_i$ changes were sufficient to induce shape changes, while gene expression required either much larger $[Ca^{2+}]_i$ signals or the combination of a smaller rise in $[Ca^{2+}]_i$ and activation

of protein kinase C. Finally, the time constant of less than 1 min for shape and motility changes contrasts dramatically with that of 90 min measured for gene expression under similar conditions. Indeed, quantitation of $[Ca^{2+}]_i$ requirements for gene expression showed that the initial $[Ca^{2+}]_i$ peak was not required for activation (Negulescu et al., 1994). Perhaps the function of the large initial $[Ca^{2+}]_i$ transient during TCR stimulation is to mediate shape changes that promote T cell recognition of the B cell.

T Cell–B Cell Contact Program

T cells contacting antigen-presenting B cells entered a reproducible program in the first 10–20 min following antigen presentation (Figure 4). The first three phases of this program are defined here as contact, recognition, and stabilization during which a T cell engages, engulfs, and partially retracts from the B cell. Our results define both spatial and temporal criteria for successful recognition of B cells by T cells. When initial T cell contact was made with the leading edge, the latency between contact and initiation of $[Ca^{2+}]_i$ signaling was as little as 25 s. This interval is similar to the lag between the addition of TCR antibodies and the $[Ca^{2+}]_i$ rise and probably represents a minimum time required to engage receptors and trigger the biochemical cascade leading to the Ca^{2+} release from internal stores (Crabtree and Clipstone, 1994). Therefore, the short latency indicates that under optimal contact conditions a T cell need only scan the B cell for a few seconds before transducing adequate information to produce a $[Ca^{2+}]_i$ rise. Proper cell–cell orientation during the first few seconds is critical since B cells placed at the trailing edge of the T cell increased this latency and greatly reduced the chance for successful engagement.

The transient engulfing of the B cell by the T cell was a defining feature of successful T cell recognition of the B cell and began prior to the $[Ca^{2+}]_i$ rise. Several factors may contribute to this phenomenon in the 1E5/2PK3 system, including the similar size of the two cell types, the roundness of the B cells, and the presence of appropriate complementary receptors and adhesion molecules on the B cell (Clark and Ledbetter, 1994; Lecomte et al., 1994). However, engulfing was also observed with α-CD3-coated beads, implying that TCR-mediated contact is sufficient to drive early T cell engulfing of the APC. Finally, in our T cell–B cell system, stable conjugates were characterized by relatively round cell pairs. Human T cell spreading following antigen presentation by L cells was reported by Donnadieu and coworkers (1994). Although we could mimic this spreading pattern with TG and phorbol myristate acetate treatment (data not shown), 1E5/2PK3 cells did not generate appropriate signal combinations to produce the spreading phenotype late in antigen presentation.

Role of $[Ca^{2+}]_i$ in T Cell–B Cell Contact during Antigen Presentation

Several findings suggest that $[Ca^{2+}]_i$ elevation causes T cell rounding during antigen presentation. First, cells with higher $[Ca^{2+}]_i$ were rounder and formed more stable pairs, and the relationship between $[Ca^{2+}]_i$ and shape in T cells engaged with B cells (Figure 5C) was similar to that of TG-treated cells (Figure 2C). Second, periods of intense signaling produced changes in T cell morphology during antigen-induced $[Ca^{2+}]_i$ oscillations. Third, blocking the $[Ca^{2+}]_i$ rise due to release of internal pools (intracellular buffering with BAPTA) and influx across the plasma membrane prevented rounding and formation of stable cell pairs. Donnadieu and Trautmann (1994) reported that activated human T cell clones make the transition from irregular scanning shapes to round immobilized shapes following $[Ca^{2+}]_i$ elevation induced by APC contact. Agarwal and Linderman (1995) have described the heterogeneity of $[Ca^{2+}]_i$ signals during antigen presentation. Our data extend these analyses and suggest that the dynamic of cell–cell contact is sensitive to the pattern of $[Ca^{2+}]_i$ signals for at least the first 30 min of interaction with the APC. Such responses by T cells could limit redundant interactions, allow other T cells access to the same B cell, and restrict T cells to the site of antigen presentation. In contrast, a weak signal would permit conjugate destabilization and limit cell activation by allowing detachment of the T cell.

Inherent T Cell Polarity

Figure 7 and Table 2 document the enhanced sensitivity to antigen at the leading edge of the T cell, a polarity that exists prior to contact with the APC. This polarity is distinct from activation-induced polarity that clusters TCR, CD4, LFA-1, and talin at the cell–cell contact plane (Kupfer et al., 1986; Kupfer and Singer, 1989) and results in cytoskeletal reorganization that requires ras-related GTPase activity (Stowers et al., 1995). Several factors could account for inherent polarity of crawling T cells. First, although the TCR and other surface molecules appear uniformly distributed before activation, there may be functional differences in those receptors due to localization of transduction elements such as G proteins, kinases, or phospholipase C at the leading edge. Indeed, protein kinase C appears enriched at the leading edge of 1E5 cells (unpublished data). The distribution of cell–cell adhesion molecules may also be polarized since B cells did not stick well to T cell tails, consistent with accumulation of anti-adhesive proteins (e.g., CD43) at the tail (Sanchez-Mateos et al., 1995). A “sticky” leading edge could help stabilize low affinity interactions between the TCR and MHC–peptide complex. Third, the motile leading edge may be more effective at engaging or aggregating enough receptors to generate an adequate signal. It is likely that the systems controlling crawling also maintain the zone of high sensitivity to antigen presentation at the leading edge. It will be of interest to investigate how specific molecular elements responsible for crawling are colocalized with the TCR or other signal transduction machinery.

Experimental Procedures

Chemicals and Solutions

Thapsigargin was obtained from LC services (Woburn, Massachusetts). All experiments were conducted in culture medium (see below). A high $[K^+]$ RPMI solution containing 90 mM $[K^+]$ (replacing Na^+) was mixed with RPMI to obtain solutions with various $[K^+]$.

Cell Culture

The murine HEL-restricted $CD4^+$ T cell (1E5) (Adorini et al., 1988) and MHC class II–restricted B cell (2PK3) hybridomas (a gift from A. Sette, Cytel) were grown in RPMI 1640 containing 10% fetal bovine serum (RPMI/FBS) 10 mM HEPES and 1% NEAA, glutamine, and Na^+ pyruvate. Cells were maintained in a humidified incubator at 37°C with 5% CO_2, 95% air. 1E5 cells were moderately adherent to plastic flasks at 37°C and were resuspended for collection by gentle shaking at room temperature. Antigen-presenting 2PK3 cells were incubated with 10 μg/ml HEL for between 3–12 hr. This protocol produced a maximal response from 1E5 T cells as judged by a contact-dependent $[Ca^{2+}]_i$ response in about 70% of cells. Peripheral human T cells from healthy donors were isolated on nylon wool columns as previously described (Hess et al., 1993) and activated by incubating with phytohemaglutinin (10 μg/ml) for 36 hr.

Video Imaging

1E5 T cells were cultured on autoclaved #0 coverglass (Red Label, Thomas Scientific, Swedesboro, New Jersey) for 4–12 hr before being loaded for 1 hr at 25°C with 3 μM fura-PE3/AM (TEFLabs, Austin, Texas), a derivative of fura-2/AM (Grynkiewicz et al., 1985) which is resistant to intracellular compartmentation and export (Vorndran et al., 1995). For experiments in which $[Ca^{2+}]_i$ was buffered, fura-loaded cells were subsequently loaded with 10 μM BAPTA/AM for 15 min at 25°C. In most T–B contact experiments, unloaded 2PK3 B cells were settled onto coverglass coated with fura-loaded T cells. In experiments where both B cell $[Ca^{2+}]_i$ was measured, fura-2-loaded B cells were settled onto unloaded T cells. Activated human T cells were loaded with fura-PE3 and settled onto poly-L-lysine (1 mg/ml) coated coverglass, since they adhered poorly to untreated glass.

Experiments were performed on a Zeiss Axiovert 35 microscope equipped with a heated stage maintained at 35°C and a custom-designed beam-splitter. The beam-splitter contained a 595 nm dichroic reflector, which directed red transmitted light from a differential interference contrast (DIC) image to a CCD camera (Sony SSC-M374) and green fluorescence emission from fura-PE3 to a low light–level SIT camera (Hamamatsu C2400). Wide-bandpass emission filters eliminated any crossover between the DIC and fluorescence images. Placement of the DIC analyzer between the splitter and the DIC camera, in a manner analogous to that described by Foskett (1988), minimized attenuation of the fluorescent signal and allowed near simultaneous detection of cell morphology and $[Ca^{2+}]_i$ with 7 s time resolution. Images were digitized, averaged (16 frames), corrected for background, stored, and analyzed by an image processor (Videoprobe, ETM Systems, Irvine, California). Experiments were conducted with either ×63 or ×100 plan Neofluor objectives. $[Ca^{2+}]_i$ was determined from the ratio of fluorescence emission intensities at 450–570 nm when exciting the dye at 360 and 380 nm. Calibration of $[Ca^{2+}]_i$ was obtained by measuring 360 of 380 ratios at zero and saturating Ca^{2+} in situ, assuming a K_d of 300 nM, and applying the equation of Grynkiewicz et al. (1985). Fura-PE3 appeared to behave ideally in T cells, yielding 360 of 380 ratios at zero and saturating Ca^{2+} of 0.7 and 7.0, respectively. Pixel ratios (512 × 512) were displayed as 8-bit pseudocolor images. The DIC/pseudocolor overlays were constructed offline by aligning the 8-bit DIC and pseudocolor images and combining them into a 24-bit look-up table. These experiments have been encoded in compressed video (MPEG) format and are available on a World Wide Web homepage by accessing our server (http://www.cell.com/Immunity). The homepage also provides links to MPEG viewers for either PC or Macintosh.

Quantitation of Cell Shape and Motility

To analyze cell shape, cell borders from DIC images of 1E5 cells and human T lymphoblasts were traced manually on a Macintosh 8100 computer using NIH Image (written by W. Rasband at the National Institutes of Health and available from the internet by anonymous ftp from zippy.nimh.nih.gov). The trace included all structures greater than ~1 μm in diameter. The DIC image has a short depth of field and represents a thin section taken near the plane of contact with glass. Cell shape in this plane was evaluated on the basis of either perimeter or circularity. Perimeter was obtained by manually tracing an outline of the T cell using NIH Image. When cells became round, the perimeter of the contact surface with glass decreased, consistent with the cell becoming spherical. A variation of the circularity-based shape index described by Donnadieu and coworkers (1992) was determined by approximating the traced shape as an ellipse using NIH image and ratioing the long and short axes; the index of a circle is 1.

The motility of 1E5 cells was analyzed by tracking the movement of the center of fura-2 fluorescence. The center was determined by averaging the position of all x and y pixel coordinates above a defined fluorescence intensity threshold. The trajectory of cell movement was plotted as consecutive x, y positions over time. Velocity was obtained by triangulating the movement of this coordinate to yield distance and dividing by the time between measurements. To reduce variability, velocity measurements represent movement averaged over three measurements (~20 s). To avoid artifacts due to cell collisions, only cells that never touched other cells were used for velocity measurements. To estimate the time that cells were immobilized following $[Ca^{2+}]_i$ elevation, we measured the time required for the cell to move 1.5 cell diameters away from its location in high $[Ca^{2+}]_i$. Human T lymphoblasts did not adhere readily to glass and were not included in measurements of motility.

Optical Trapping

Antigen-presenting B (2PK3) cells or beads coated with α-CD3 monoclonal antibody were micromanipulated into contact at various points on a T cell using a tunable near infra-red titanium–sapphire laser (Coherent) producing a trapping beam at about 760 nm (Berns et al., 1992). The laser was directed through the TV port of a modified Axiovert 135 microscope, past a custom short-pass (720 nm) dichoic reflector and a ×63 Neofluor objective and produced about 60 mW trapping power at the focal plane. The microscope was also equipped with a Zeiss Laser Scanning Confocal (LSM 410) with an argon laser set at 488 nm. This arrangement allowed both trapping and $[Ca^{2+}]_i$ measurements on the same cells. To measure T cell $[Ca^{2+}]_i$ on the LSM 410, 1E5 cells were coloaded with a combination of fura-red/AM (5 μM) and fluo-3/AM (2 μM), two long-wavelength Ca^{2+} indicators that respond to the 488 nm excitation line of the argon laser. Cells loaded for 1 hr at 25°C produced a red to green emission shift when $[Ca^{2+}]_i$ was elevated (Diliberto et al., 1994). This shift was quantitated by scanning cells with the argon laser and dividing the fluorescence intensity signals from two photomultipliers with emission bands of 535–585 nm (green) and >610 nm (red). In these experiments a single 2PK3 cell was held in the trap on a heated stage and positioned so that it made contact with a particular region of a dye-loaded T cell. Once the cells were positioned, the trapping beam was cut off and 488 nm laser excitation scans were performed to monitor $[Ca^{2+}]_i$. A third photomultiplier collected a Ca^{2+}-insensitive blue emission band (400–480 nm) from incandescent illumination, which was used to produce a brightfield image. Therefore, the final red–green–blue image contained fura-red intensity in the red channel, fluo-3 intensity in the green channel, and a grey scale brightfield image in the blue channel. We made 30–40 scans at 10 s intervals to determine whether a $[Ca^{2+}]_i$ increase occurred in the T cell following contact with the APC. T cells not responding within 400 s were scored as unresponsive. Because the B cell was between one-third to one-half the size of the T cell, the spatial resolution of mapping was about a third of the length of the T cell (~5 μm). For trapping experiments with beads, we used 6 μm diameter polystyrene microspheres stabilized with sulfate charges (IDC, Portland, Oregon). Goat α-rat immunoglobulin G (100 μg/ml) (Zymed Laboratories, South San Francisco, California) in 10% PBS was adsorbed to beads (0.5% solids) for 8 hr at room temperature, centrifuged, and washed twice with 10% PBS and then conjugated with 50 μg/ml rat α-mouse CD3ε for 3 hr. Beads were centrifuged and washed twice before use. Beads were active (i.e., able to stimulate T cells) for up to 8 weeks when stored at 4°C.

Acknowledgments

Correspondence should be addressed to M. D. C. This work was supported by National Institutes of Health grants GM41514 and NS14609 (M. D. C.), and by a Schrodinger Stipendium (H. H. K.).

Optical trap experiments were performed at the Laser Microbeam and Medical Program and the Optical Biology Shared Resource Facility of the Clinical Cancer Center, supported by National Institutes of Health grants RR-01192 and CA-62203. We thank A. Sette for providing 1E5 and 2PK3 cell hybridomas, B. Tromberg for supporting optical trap experiments, S. Hess and D. Choquet for initiating studies on T–B contact, L. Forrest for tissue culture support, Y. Osipchuk for drafting plans for the two-camera beam-splitter, P. Steinbach for video software support, P. Ross, G. Ehring for helpful discussions, and A. Lepple-Weinhues for establishing and maintaining our Internet server.

Received March 13, 1996; revised April 2, 1996.

References

Adorini, L., Sette, A., Buus, S., Grey, H.M., Darsley, M., Lehman, P.V., Doria, G., Nagy, Z.A., and Appella, E. (1988). Interaction of an immunodominant epitope with Ia molecules in T cell activation. Proc. Natl. Acad. Sci. USA *85*, 5181–5185.

Agarwal, N.G.B., and Linderman, J.L. (1995). Calcium response of helper T lymphocytes to antigen-presenting cells in a single-cell assay. Biophys. J. *69*, 1178–1190

Arencibia, I., Pedari, L., and Sundqvist, K.-G. (1987). Induction of motility and alteration of surface membrane polypeptides in lymphocytes in contact with autologous and allogenic fibroblasts. Exp. Cell Res. *172*, 124–133.

Berns, M.W., Aist, J.R., Wright, W.H., and Liang, H. (1992). Optical trapping in animal and fungal cells using a tunable, near-infrared titanium–sapphire laser. Exp. Cell Res. *198*, 375–378.

Brundage, R.A., Fogarty, K.E., Tuft, R.A., and Fay, F.S. (1991). Calcium gradients underlying polarization and chemotaxis of eosinophils. Science *254*, 703–706.

Clark, E.A., and Ledbetter, J.A. (1994). How B and T cells talk to each other. Nature *367*, 425–426.

Crabtree, G.R., and Clipstone, N.A. (1994). Signal transmission between the plasma membrane and nucleus in T lymphocytes. Annu. Rev. Biochem. *63*, 1045–1083.

del Pozo, M.A., Sanchez-Mateos, P., Nieto, M., and Sanchez-Madrid, F. (1995). Chemokines regulate cellular polarization and adhesion receptor distribution during lymphocyte interaction with endothelium and extracellular matrix: involvement of cAMP signaling pathway. J. Cell Biol. *131*, 495–508.

Diliberto, P.A., Wang, X.F., and Herman, B. (1994). Confocal imaging of Ca^{2+} in cells. Meth. Cell Biol. *40*, 243–262.

Donnadieu, E., Cefai, D., Tan, Y.P., Paresys, G., Bismuth, G., and Trautmann, A. (1992). Imaging early activation events in human T cell activation by antigen presenting cells. J. Immunol. *148*, 2643–2653.

Donnadieu, E., Bismuth, G., and Trautmann, A. (1994). Antigen recognition by helper T cells elicits a sequence of distinct changes of their shape and intracellular calcium. Curr. Biol. *4*, 584–595.

Foskett, J.K. (1988). Simultaneous Nomarski and fluorescence imaging during video microscopy of cells. Am. J. Physiol. *255*, C566-C571.

Gouy, H., Cefai, D., Christensen, S.B., Debre, P., and Bismuth, G. (1990). Ca^{2+} influx in human T lymphocytes is induced independently of inositol phosphate production by mobilization of intracellular Ca^{2+} stores: a study with the endoplasmic reticulum Ca^{2+}–ATPase inhibitor thapsigargin. Eur J. Immunol. *20*, 2269–2275.

Grynkiewicz, G., Poenie, M., and Tsien., R.Y. (1985). A new generation of calcium-sensitive fluorescent indicators. J. Biol. Chem. *260*, 3440–3448.

Hendey, B., Klee, C.B., and Maxfield, F.R. (1992). Inhibition of neutrophil chemokinesis by inhibitors of calcineurin. Science *258*, 296–299.

Hess, S.D., Oortgiesen, M., and Cahalan, M.D. (1993). Calcium oscillations in human T and natural killer cells depend upon membrane potential and calcium influx. J. Immunol. *150*, 2620–2633.

Kupfer, A., and Singer, S.J. (1989). Cell biology of cytotoxic and helper T cell functions. Annu. Rev. Immunol. *7*, 309–337.

Kupfer, A., Swain, S.L., Janeway, C.A., Jr., and Singer, S.J. (1986). The specific direct interaction of helper T cells and antigen-presenting B cells. Proc. Natl. Acad. Sci. USA *83*, 6080–6083.

Kupfer, H., Monks, C.R.F., and Kupfer, A. (1994). Small splenic B cells that bind to antigen-specific T helper (Th) cells and face the site of cytokine production in the Th cells selectively proliferate. J. Exp. Med. *179*, 1507–1515.

Lecomte, O., Haus, P., Barbat, C., Mazerolles, F., and Fischer, A. (1994). Role of LFA-1, CD2, VLA-5/CD29 and CD43 surface receptors in $CD4^+$ T cell adhesion to B cells. Cell. Immunol. *158*, 376–388.

Lee, J.T., Black, J.D., Repasky, E.A., Kubo, R.T., and Bankert, R.B. (1988). Activation induces a rapid reorganization of spectrin in lymphocytes. Cell *55*, 807–816.

Mandeville, J.T.H., Ghosh, R.N., and Maxfield, F.R. (1995). Intracellular calcium levels correlate with speed and persistent forward motion in migrating neutrophils. Biophys. J. *68*, 1207–1217.

Maxfield, F.R. (1993). Regulation of leukocyte locomotion by Ca^{2+}. Trends Cell Biol. *3*, 386–391.

Negulescu, P.A., Shastri, N., and Cahalan, M.D. (1994). $[Ca^{2+}]_i$ dependence of gene expression in single T lymphocytes. Proc. Natl. Acad. Sci. USA *91*, 2873–2877.

Poo, W.J., Conrad, L., and Janeway, C.A., Jr. (1988). Receptor-directed focusing of lymphokine release by helper T cells. Nature *332*, 378–80.

Sanchez-Mateos, P., Campanero, M.R., del Pozo, M.A., and Sanchez-Madrid, F. (1995). Regulatory role of CD43 leukosialin on integrin-mediated T cell adhesion to endothelial and extracellular matrix ligands and its polar redistribution to a cellular uropod. Blood *86*, 2238–2239

Shimizu, Y., and Shaw, S. (1991). Lymphocyte interactions with extracellular matrix. FASEB J. *5*, 2292–2299

Sjaastad, M.D., Angres, B., Lewis, R.S., and Nelson, W.J. (1994). Feedback regulation of cell-substratum adhesion by integrin-mediated intracellular Ca^{2+} signaling. Proc. Natl. Acad. Sci. USA *91*, 8214–821.

Springer, T.A. (1994). Traffic signals for lymphocyte recirculation and leukocyte emigration: a multi-step paradigm. Cell *76*, 310–314

Stossel, T.P. (1993). On the crawling of animal cells. Science *260*, 1086–1094.

Stowers, L., Yelon, D., Berg, L.J., and Chant, J. (1995). Regulation of the polarization of T cells toward antigen-presenting cells by Ras-related GTPase CDC42. Proc Natl. Acad. Sci. USA *92*, 5027–5031.

Tan, J., Deleuran, B., Gesser, B., Maare, H., Deleuran, M., Larsen, C.G., and Thestrup-Pedersen, K. (1995). Regulation of human T lymphocyte chemotaxis in vitro by T cell–derived cytokines IL-2, IFN-gamma, IL-4, IL-10, and IL-13. J. Immunol. *154*, 3742–52.

Thastrup, O., Dawson, A.P., Scharff, O., Foder, B., Cullen, P.J., Drobak, B.K., Bjerrum, P.J., Christensen, S.B., and Hanley, M.R. (1989). Thapsigargin, a novel molecular probe for studying intracellular calcium release and storage. Agents Act. *27*, 17–23.

Thorpe, K.M., Southern, C., and Matthews, N. (1994). Effect of serine/threonine kinase inhibitors on motility of human lymphocytes and U937 cells. Immunology *81*, 546–550.

Vorndran, C., Minta, A., and Poenie, M. (1995). New fluorescent calcium indicators designed for cytosolic retention or measuring calcium near membranes. Biophys. J. *69*, 2112–2124

Zweifach, A., and Lewis, R.S. (1993). Mitogen-regulated Ca^{2+} current of T lymphocytes is activated by depletion of intracellular Ca^{2+} stores. Proc. Natl. Acad. Sci. USA *90*, 6295–6299.